JOURNAL OF GUIDANCE, CONTROL, AND DYNAMICS
Vol. 28, No. 1, January–February 2005

Control of Unsteady Aeroelastic System via State-Dependent Riccati Equation Method

Nilesh Bhoir* and Sahjendra N. Singh†
University of Nevada, Las Vegas, Nevada 89154-4026

A nonlinear control system for the flutter control of an aeroelastic system with unsteady aerodynamics is designed. The model describes the plunge and pitch motion of a wing. In this model both plunge and pitch structural nonlinearities are included. A single control surface is utilized for the flutter control. For the purpose of design, it is assumed that there exists a specified hard magnitude constraint on the control input. For the synthesis of the controller, only the plunge displacement, pitch angle, and control-surface deflection are measured. The control system design is based on the state-dependent Riccati equation method. A slack variable is introduced to transform the constrained control problem into an unconstrained problem and then a suboptimal nonlinear control law is designed. An observer is constructed to estimate the unavailable state variables of the system for the synthesis of the control system. In the closed-loop system, including the observer and nonlinear controller, the zero state is (locally) asymptotically stable, and the state vector asymptotically converges to the origin. Simulation results for various flow velocities and elastic axis locations are presented, which show that the designed control system is effective in flutter suppression.

Nomenclature

A_a, B_a, A, B	=	system matrices
a	=	nondimensionalized distance from the midchord to the elastic axis
b	=	semichord of the wing
$C(k)$	=	Theodorsen's function
C_m	=	measurement matrix
c_h	=	plunge degree of freedom structural damping coefficient
c_α	=	pitch degree of freedom structural damping coefficient
F_0	=	observer gains
h	=	plunge displacement coordinate
I_α	=	mass moment of inertia about the elastic axis
J, J_a	=	performance indices
k	=	reduced frequency $(b\omega/u_\infty)$
k_h	=	plunge degree of freedom structural spring constant
k_α	=	pitch degree of freedom structural spring constant
$L(t)$	=	lift of the wing
$M(t)$	=	moment of the wing about the elastic axis
m_w	=	mass of the wing
P_a	=	matrix satisfying the Riccati equation
Q_0, R_0, Q_a, R, ϵ	=	weighting matrices
U_n	=	new control input
u	=	freestream velocity
v_f, y_f	=	filter input, output
x, y	=	state vector, output variable
x_a, x_s	=	augmented state vector, slack variable
x_α	=	nondimensional distance between elastic axis and center of mass
y_m	=	measured output vector
α	=	pitch displacement coordinate
β	=	control-surface-deflection coordinate
β_c	=	control input
β_{cm}	=	maximum control-surface-deflection coordinate
ρ	=	density of air
ω	=	frequency of motion

Received 19 November 2003; revision received 4 January 2004; accepted for publication 5 January 2004.

*Graduate Student, Department of Electrical and Computer Engineering.
†Professor, Department of Electrical and Computer Engineering. Associate Fellow AIAA.

I. Introduction

AEROELASTIC systems exhibit a variety of phenomena including instability, limit cycles, and even chaotic vibration.[1–3] Researchers in aerodynamics, structure, materials, and control have made important contributions to the analysis and control of aeroelastic systems. Readers may refer to Ref. 3 for an excellent historical perspective on analysis and control of aeroelastic responses. Analysis of stability properties of aeroelastic systems and design of controllers for flutter suppression have been considered in Refs. 4–26. Robust aeroservoelastic stability margins using the μ method have been obtained.[4] Digital adaptive control of a linear aeroservoelastic model has been considered.[5] At the NASA Langley Research Center, a benchmark active-control technology (BACT) wind-tunnel model has been designed and control algorithms for flutter suppression have been developed.[6–11] References 7 and 8 describe unsteady aerodynamic data and flutter instability for the BACT project model. The classical and minmax methods were used to derive robust flutter-control systems.[9] Robust passivation techniques were used in Ref. 10 for control. Gain scheduled controllers were designed in Ref. 11. Neural and adaptive control of transonic wind-tunnel models were considered.[12,13] Based on the Euler–Lagrange theory, a control law for an aeroelastic model was presented.[14] For an aeroelastic apparatus, tests were performed in a wind tunnel to examine the effect of nonlinear structural stiffness and control systems were designed using linear control theory, feedback linearizing techniques, and adaptive control strategies.[15–26] A model reference variable structure adaptive control system for plunge displacement and pitch-angle control was designed using bounds on uncertain functions.[22] This approach yields a high-gain feedback discontinuous control system. A backstepping adaptive design method for flutter suppression was adopted in Refs. 23 and 24. In this approach, the aeroelastic model was represented in an output feedback form by suitable coordinate transformation and output feedback adaptive laws were derived. A modular adaptive flutter-control system was designed in Ref. 25. The control system consisted of an input-to-state stabilizing controller and a passive identifier. The state-dependent

Riccati equation (SDRE) method was advanced in a series of papers and applied to solve a variety of aerospace control problems.[27–30] Based on the SDRE method, suboptimal control laws for flutter suppression were designed.[31,32]

The feedback designs of Refs. 17–20, 22–25, 31, and 32 assume aeroelastic models with quasi-steady aerodynamics. Active output feedback control of an aeroelastic system with unsteady aerodynamics was considered using a linear quadratic regulator (LQR) approach in Ref. 16. Of course, linear design ignores the nonlinearity in the aeroelastic model. A feedback linearizing control law for a minimum-phase model with unsteady aerodynamics was obtained in Ref. 26, but this method cannot be applied at those flow velocities and elastic axis locations for which the system has unstable zero dynamics (that is, the system is non-minimum-phase). Thus, it is of interest to explore the applicability of the SDRE method to flutter control for nonlinear aeroelastic models with unsteady aerodynamics and unstable zero dynamics.

The contribution of this paper lies in the derivation of a nonlinear output feedback control law for the flutter control of an aeroelastic model that includes unsteady aerodynamics. The model has both plunge and pitch structural nonlinearities. The unsteady aerodynamics are modeled with an approximation to Theodorsen's theory.[33] The model represents a prototypical aeroelastic wing section that has traditionally been used for the theoretical and experimental study of two-dimensional aeroelastic behavior. A single trailing-edge control surface is used for the control of the system. For the purpose of design, it is assumed that the control input is limited, and therefore a hard constraint is imposed on the control magnitude. It is assumed that only the plunge displacement, pitch angle, and control-surface deflection are measured for feedback. Based on the SDRE method, a nonlinear suboptimal control law is designed for flutter control. An observer is designed to construct the state variables associated with the Theodorsen function as well as the derivatives of the measured variables for the synthesis of the control system. The closed-loop aeroelastic system including the nonlinear controller is locally asymptotically stable about the origin in the state space. Simulation results are presented which show that the plunge and pitch angle trajectories converge to the origin for large perturbations in the initial state vector in spite of the hard magnitude constraint on control input.

The organization of the paper is as follows. Section II presents the aeroelastic model. An observer and a feedback control law are designed in Sec. III, and Sec. IV presents simulation results.

II. Aeroelastic Model and Control Problem

The prototypical aeroelastic wing section is shown in Fig. 1.

A. Mathematical Model

The governing equations of motion, provided in Refs. 16–20, are given by

$$\begin{bmatrix} m_t & m_w x_\alpha b \\ m_w x_\alpha b & I_\alpha \end{bmatrix}\begin{bmatrix} \ddot{h} \\ \ddot{\alpha} \end{bmatrix} + \begin{bmatrix} c_h & 0 \\ 0 & c_\alpha \end{bmatrix}\begin{bmatrix} \dot{h} \\ \dot{\alpha} \end{bmatrix} + \begin{bmatrix} k_h(h) & 0 \\ 0 & k_\alpha(\alpha) \end{bmatrix}\begin{bmatrix} h \\ \alpha \end{bmatrix} = \begin{bmatrix} -L(t) \\ M(t) \end{bmatrix} \tag{1}$$

The lift $L(t)$ and moment $M(t)$, which represent the unsteady aerodynamics, are functions of position, velocity, acceleration, and time. The lift and moment are acting at the elastic axis of the wing. For purposes of illustration, the function $k_\alpha(\alpha)$ and $k_h(h)$ are considered as polynomial nonlinearities of fourth and second degree, respectively. These are given by

$$\alpha k_\alpha(\alpha) = \alpha\left(k_{\alpha_0} + k_{\alpha_1}\alpha + k_{\alpha_2}\alpha^2 + k_{\alpha_3}\alpha^3 + k_{\alpha_4}\alpha^4\right) \doteq k_{\alpha_0}\alpha + k_{n_\alpha}(\alpha) \tag{2}$$

$$h k_h(h) = h\left(k_{h_0} + k_{h_1}h^2\right) \doteq h k_{h_0} + k_{n_h}(h) \tag{3}$$

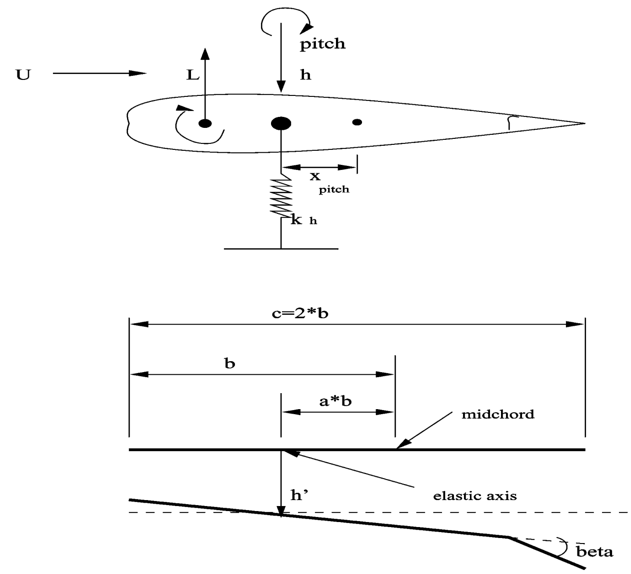

Fig. 1 Aeroelastic model.

Theodorsen[33] derived expressions for lift and moment, assuming harmonic motion of the airfoil, of the form[16]

$$-L(t) = -\rho b^2 s_p(u\pi\dot{\alpha} + \pi\ddot{h} - \pi b a\ddot{\alpha} - uT_4\dot{\beta} - T_1 b\ddot{\beta}) - 2\pi\rho u b s_p C(k)\left[u\alpha + \dot{h} + b\left(\tfrac{1}{2} - a\right)\dot{\alpha} + (1/\pi)T_{10}u\beta + b(1/2\pi)T_{11}\dot{\beta}\right] \tag{4}$$

$$M(t) = -\rho b^2 s_p\Big\{\pi\left(\tfrac{1}{2} - a\right)u b\dot{\alpha} + \pi b^2\left(\tfrac{1}{8} + a^2\right)\ddot{\alpha} + (T_4 + T_{10})u^2\beta + \left[T_1 - T_8 - (c - a)T_4 + \tfrac{1}{2}T_{11}\right]u b\dot{\beta} - [T_7 + (c - a)T_1]b^2\ddot{\beta} - a\pi b\ddot{h}\Big\} + 2\rho u b^2\pi s_p\left(\tfrac{1}{2} + a\right)C(k) \left[u\alpha + \dot{h} + b\left(\tfrac{1}{2} - a\right)\dot{\alpha} + (1/\pi)T_{10}u\beta + b(1/2\pi)T_{11}\dot{\beta}\right] \tag{5}$$

where $T_i(i = 1, 4, 7, 8, 10, 11)$ are described by Theodorsen and depend on the elastic axis location and the control-surface hinge location. The Theodorsen function $C(k)$ is a complex function of the form[16]

$$C(k) = F(k) + jG(k) \tag{6}$$

where k is the reduced frequency $(b\omega/u)$ and $F(k)$ and $G(k)$ are composed of Bessel functions. Jones developed an approximation to Theodorsen's function for simplicity in computation, which can be written as[16]

$$C(s) = 1 - \frac{0.0165s}{s + 0.0455(u/b)} - \frac{0.335s}{s + 0.3(s/b)} \tag{7}$$

$$\doteq 0.5 + \frac{a_1 s + a_0}{s^2 + b_1 s + b_0} \tag{8}$$

where s is the Laplace variable and

$$a_1 = 0.1080075(u/b), \qquad a_0 = 0.006825(u^2/b^2)$$

$$b_1 = 0.3455(u/b), \qquad b_0 = 0.01365(u^2/b^2)$$

The control surface dynamics are described by[16]

$$\ddot{\beta} + b_{c1}\dot{\beta} + b_{c0}\beta = b_{c0}\beta_c \tag{9}$$

where $b_{c1} = 50$, $b_{c0} = 2500$, and β_c is the control input to the aeroelastic model.

B. State Variable Representation

It will be convenient to obtain a state variable form of the complete model. The Theodorsen function $C(s)$ can be treated as a second-order transfer function of a filter with input

$$v_f(t) = [u\alpha + \dot{h} + b(0.5 - a)\dot{\alpha} + (1/\pi)T_{10}u\beta + b(1/2\pi)T_{11}\dot{\beta}] \doteq \boldsymbol{a}_v^T \boldsymbol{x}_p \tag{10}$$

where the vector $\boldsymbol{a}_v \in R^6$ is

$$\boldsymbol{a}_v = [0, u, 1/\pi T_{10}u, 1, b(5 - a), b(1/2\pi)T_{11}]^T \tag{11}$$

and the partial state vector is $\boldsymbol{x}_p = (h, \alpha, \beta, \dot{h}, \dot{\alpha}, \dot{\beta})^T \in R^6$. The output of the filter is denoted as $y_f(t)$, which is related to the input $v_f(t)$ as

$$\hat{y}_f(s) = C(s)\hat{v}_f(s) \tag{12}$$

where $\hat{y}_f(s)$ and $\hat{v}_f(s)$ represent Laplace transforms of $y_f(t)$ and $v_f(t)$, respectively. We note that the input to the filter $C(s)$ is a linear combination of the plunge, pitch, and control-surface-deflection variables.

The transfer function $C(s)$ of the filter has a minimal realization of dimension 2. Although one can derive a variety of realizations of $C(s)$, we consider a representation of the filter of the form

$$\dot{x}_{f1} = x_{f2}, \qquad \dot{x}_{f2} = -b_0 x_{f1} - b_1 x_{f2} + v_f \tag{13}$$

with its output given by

$$y_f = 0.5v_f + a_0 x_{f1} + a_1 x_{f2} = 0.5a_v^T x_p + a_0 x_{f1} + a_1 x_{f2} \tag{14}$$

In view of Eqs. (12) and (14), $L(t)$ and $M(t)$ [Eqs. (4) and (5)] can be written as

$$-L(t) = \left[-\rho b^2 s_p(u\pi\dot{\alpha} - uT_4\dot{\beta} - T_1 b\ddot{\beta}) - 2\pi\rho s_p u b y_f\right] - \pi\rho b^2 s_p(\ddot{h} - ba\ddot{\alpha}) \tag{15}$$

$$M(t) = \Big(-\rho b^2 s_p\big\{\pi(0.5 - a)ub\dot{\alpha} + (T_4 + T_{10})u^2\beta + \left[T_1 - T_8 - (c - a)T_4 + \tfrac{1}{2}T_{11}\right]ub\dot{\beta} - [T_7 + (c - a)T_1]b^2\ddot{\beta}\big\} + 2\pi\rho s_p u b^2(0.5 + a)y_f\Big) + b^3\rho s_p\pi\left[a\ddot{h} - b\left(\tfrac{1}{8} + a^2\right)\ddot{\alpha}\right] \tag{16}$$

Define the state vector, including the filter states, as

$$\boldsymbol{x} = (h, \alpha, \beta, \dot{h}, \dot{\alpha}, \dot{\beta}, x_{f1}, x_{f2})^T \in R^8 \tag{17}$$

Substituting $\ddot{\beta} = -b_{c1}\dot{\beta} - b_{c0}(\beta - \beta_c)$ from Eq. (9) and y_f from Eq. (14) into Eqs. (15) and (16), one can express the terms in the square brackets as linear functions of x and β_c. Substituting the resulting expressions of L and M into Eq. (1), collecting the terms involving $\ddot{h}$ and $\ddot{\alpha}$, solving for $\ddot{h}$ and $\ddot{\alpha}$, and using Eq. (9) gives

$$\begin{bmatrix} \ddot{h} \\ \ddot{\alpha} \\ \ddot{\beta} \end{bmatrix} = A_1\boldsymbol{x} + B_1\beta_c + N_1 f_n(h, \alpha) \tag{18}$$

for appropriate matrices $A_1 \in R^{3\times 8}$ and $B_1 \in R^3$, where f_n denotes the structural nonlinearities, $f_n(h, \alpha) = [h_{nh}(h), k_{n\alpha}(\alpha)]^T$, $N_1 = [-M_a^{-1}, 0_{2\times 1}]^T$, and the matrix M_a is

$$M_a = \begin{bmatrix} m_t + \pi\rho b^2 s_p & m_w x_\alpha b - \pi\rho b^3 a s_p \\ m_w x_\alpha b - \pi\rho b^3 a s_p & I_\alpha + \pi\rho b^4 s_p(1/8 + a^2) \end{bmatrix} \tag{19}$$

The complete system, including Eqs. (9), (13), and (18), has a state variable representation of the form

$$\frac{\mathrm{d}}{\mathrm{d}t}\begin{bmatrix} h \\ \alpha \\ \beta \\ \dot{h} \\ \dot{\alpha} \\ \dot{\beta} \\ \dot{x_{f1}} \\ \dot{x_{f2}} \end{bmatrix} = \begin{bmatrix} O_{3\times 3} & I_{3\times 3} & O_{3\times 2} \\ & A_1 & \\ O_{1\times 7} & 1 & \\ \boldsymbol{a}_v & -b_0 & -b_1 \end{bmatrix}\boldsymbol{x} + \begin{bmatrix} O_{3\times 1} \\ B_1 \\ 0 \\ 0 \end{bmatrix}\beta_c + \begin{bmatrix} 0_{3\times 2} \\ N_1 \\ 0 \\ 0 \end{bmatrix} f_n(h, \alpha) \doteq A\boldsymbol{x} + B\beta_c + N f_n(h, \alpha) \tag{20}$$

where O and I denote null and identity matrices of indicated dimensions.

It is assumed that the control input is constrained as

$$|\beta_c(t)| \le \beta_{\text{cm}} \tag{21}$$

where β_{cm} is the maximum permissible magnitude of the control input β_c.

The measurement equation is

$$\boldsymbol{y}_m = [h, \alpha, \beta]^T \doteq C_m\boldsymbol{x} \tag{22}$$

where

$$C_m = [I_{3\times 3} O_{3\times 5}]$$

We are interested in designing an output feedback control law satisfying the bound given in Eq. (21) such that in closed-loop systems, both the pitch angle and the plunge displacement asymptotically converge to zero.

III. Control Law Design

In this section, the derivation of a nonlinear controller is considered.

A. Observer Design

First, it is essential to construct an observer so that unavailable state variables $(\dot{h}, \dot{\alpha}, \dot{\beta}, x_{f1}, x_{f2})$ can be estimated. Noting that h, α, and β are available, one can construct a full-order observer of the form

$$\dot{\hat{\boldsymbol{x}}} = A\hat{\boldsymbol{x}} + B\beta_c + N f_n(h, \alpha) + F_0(\boldsymbol{y}_m - \hat{\boldsymbol{y}}_m) \tag{23}$$

where $\hat{\boldsymbol{x}}$ denotes estimated values of the state vector $\boldsymbol{x}$, F_0 is a 8×3 matrix, and $\hat{\boldsymbol{y}}_m = (\hat{h}, \hat{\alpha}, \hat{\beta})^T = C_m\hat{\boldsymbol{x}}$. After Eq. (23) is subtracted from Eq. (20), it easily follows that the state estimation error $\tilde{\boldsymbol{x}} = \boldsymbol{x} - \hat{\boldsymbol{x}}$ satisfies

$$\dot{\tilde{\boldsymbol{x}}} = (A - F_0 C_m)\tilde{\boldsymbol{x}} \doteq A_c\tilde{\boldsymbol{x}} \tag{24}$$

For the convergence of the estimation error to zero, one computes F_0 such that the matrix $A_c = (A - F_0 C_m)$ is Hurwitz (i.e., its eigenvalues have negative real parts). For this purpose one can use the pole placement or LQR design approach. Here in this study, F_0 has been obtained using the LQR technique[34] by minimizing the quadratic performance index

$$J = \frac{1}{2}\int_0^\infty \left(z^T Q_0 z + \boldsymbol{u}_0^T R_0 \boldsymbol{u}_0\right)\mathrm{d}t \tag{25}$$

for a related system $\dot{\boldsymbol{z}} = A^T\boldsymbol{z} + C_m^T\boldsymbol{u}_0$, where Q_0 and R_0 are the positive definite symmetric weighting matrices. Then

$$F_0 = -\left(R_0^{-1} C_m P_0\right)^T \tag{26}$$

where P_0 satisfies the Riccati equation

$$AP_0 + PA^T + Q_0 - P_0 C_m^T R_0^{-1} C_m P_0 = 0 \quad (27)$$

For this value of F_0, A_c is a Hurwitz matrix. Therefore, the origin ($\tilde{\boldsymbol{x}} = 0$) of Eq. (24) is exponentially stable and $\tilde{x}(t)$ converges to zero. Thus the observer accomplishes state estimation.

Now the design of a suboptimal control system for the regulation of the state vector to the origin is considered.

B. State Variable Feedback Control Law

This section describes a nonlinear control law based on the SDRE method[27–30] for flutter control, assuming that the control input is constrained. The design of flutter control is applicable even if both matrices A and B are nonlinear functions of the state vector $\boldsymbol{x}$. Of course, for the model under consideration, matrix B is a constant matrix.

The SDRE method is suitable for the design of the controller even when there is a hard constraint on the input β_c. Following Ref. 28, the bounded control problem is transformed to an equivalent nonlinear regulator problem by introducing a slack variable x_s that satisifes

$$\dot{x}_s = U_n \quad (28)$$

where U_n is a new control input and β_c takes the form of a saturation sin function, given by

$$\beta_c = \text{satsin}(\beta_{\text{cm}}, x_s) \quad (29)$$

where one defines

$$\text{satsin}(\beta_{\text{cm}}, x_s) = \begin{cases} \beta_{\text{cm}} & \text{for} \quad x_s > \pi/2 \\ \beta_{\text{cm}} \sin x_s & \text{for} \quad -\pi/2 \le x_s \le -\pi/2 \\ -\beta_{\text{cm}} & \text{for} \quad x_s < -\pi/2 \end{cases} \quad (30)$$

According to the definition of the satsin function, the control input, which is a function of the output x_s of an integrator, satisfies the magnitude constraint for any value of x_s. Of course, the new control variable U_n, which is the input to the integrator, is unconstrained.

Define the augmented state vector as $\boldsymbol{x}_a = (\boldsymbol{x}^T, x_s)^T \in R^9$. Then using Eqs. (20), (28), and (29), the derivative of $\boldsymbol{x}_a$ can be written as

$$\dot{\boldsymbol{x}}_a = A_a(\boldsymbol{x}_a)\boldsymbol{x}_a + B_a U_n \quad (31)$$

where

$$A_a = \begin{bmatrix} A & B\dfrac{\text{satsin}(\beta_{\text{cm}}, x_s)}{x_s} \\ 0_{1\times 8} & 0 \end{bmatrix}, \qquad B_a = \begin{bmatrix} 0_{8\times 1} \\ 1 \end{bmatrix} \quad (32)$$

Consider an optimal control (infinite-horizon regulator) problem in which, for the nonlinear system, the performance index of the form

$$J_a = \frac{1}{2}\int_0^\infty \left(\boldsymbol{x}_a^T Q_a \boldsymbol{x}_a + \epsilon U_n^2\right) \mathrm{d}t \quad (33)$$

where

$$Q_a = \begin{bmatrix} Q & 0_{8\times 1} \\ 0_{1\times 8} & Rq_q \end{bmatrix} \quad (34)$$

$$q_q = \begin{cases} \dfrac{[\text{satsin}(\beta_{\text{cm}}, x_s)/x_s]^2}{x_s}, & |x_s| \le \pi/2 \\ \dfrac{\beta_{\text{cm}}}{x_s}, & |x_s| \le \pi/2 \end{cases} \quad (35)$$

is to be minimized. Here $Q(\boldsymbol{x})$ is a positive definite symmetric matrix and $R > 0$ for all $\boldsymbol{x}_a \in R^9$. The weighting matrix $Q_a(\boldsymbol{x}_a)$ and the scalar function $\epsilon > 0$ are chosen properly for obtaining desirable responses in the closed-loop system. Instead of deriving an optimal control law, for simplicity, a suboptimal control law is designed using the SDRE method.

Consider a region of interest $\Omega_a \in R^9$ of the state space surrounding the origin $\boldsymbol{x}_a = 0$. For the existence of a solution using the SDRE method, the pair $\{A_a(\boldsymbol{x}_a), B_a\}$ must be pointwise stabilizable at each $\boldsymbol{x}_a \in \Omega$.[30] For the linearized aeroelastic model, it is found that the rank of the controllability matrix

$$\left[B_a, A_a(0)B_a, \ldots, A_a^8(0)B_a\right]$$

is 9, and therefore the system is controllable. This also implies that the system is pointwise controllable in a neighborhood of the origin. Indeed simulation results of Section 4 confirm that the controllability matrix of the pair $\{A_a(\boldsymbol{x}), B_a\}$ has rank 9 at each x along the closed-loop trajectory of the system and the solution of the Riccati equation exists.

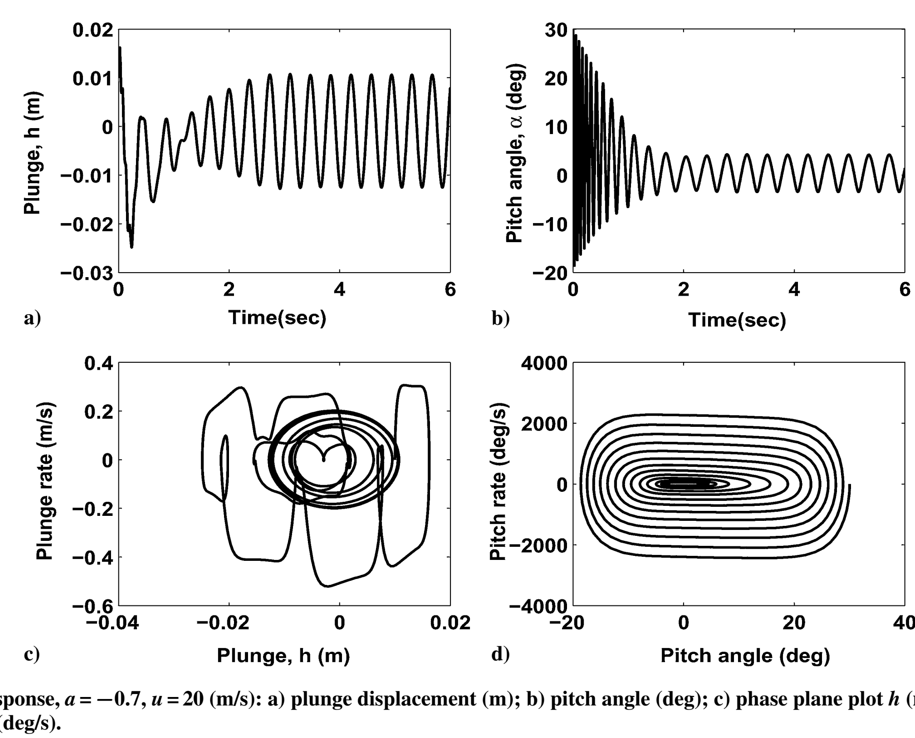

Fig. 2 Open-loop response, $a = -0.7$, $u = 20$ (m/s): a) plunge displacement (m); b) pitch angle (deg); c) phase plane plot h (m)–$\dot{h}$ (m/s); and d) phase plane plot α (deg)–$\dot{\alpha}$ (deg/s).

Now, for obtaining a suboptimal solution using the SDRE method,[28] one solves the state-dependent Riccati equation given by

$$A_a^T(\boldsymbol{x}_a)P(\boldsymbol{x}_a) + P(\boldsymbol{x}_a)A_a(\boldsymbol{x}_a) - P(\boldsymbol{x}_a)B_a\epsilon^{-1}B_a^T P(\boldsymbol{x}_a) + Q_a(\boldsymbol{x}_a) = 0 \tag{36}$$

to obtain a symmetric positive definite solution for $P(\boldsymbol{x}_a)$. Then the nonlinear feedback control law is given by

$$U_n(x_a) = -\epsilon^{-1}B_a^T P(\boldsymbol{x}_a)\boldsymbol{x}_a \tag{37}$$

Readers may refer to Ref. 30 for the properties and capabilities of the SDRE method. It is interesting to note that the suboptimal law satisfies

$$\frac{\mathrm{d}H(\boldsymbol{x}_a, \lambda)}{\mathrm{d}U_n} = 0 \tag{38}$$

where the Hamiltonian of the nonlinear optimal-control problem is

$$H(\boldsymbol{x}_a, \boldsymbol{\lambda}) = \tfrac{1}{2}\left[\boldsymbol{x}_a^T Q_a(\boldsymbol{x}_a)\boldsymbol{x}_a + \epsilon^{-1}U_n^2\right] + \boldsymbol{\lambda}^T[A_a(\boldsymbol{x}_a)\boldsymbol{x}_a + B_a U_c] \tag{39}$$

and $\lambda \in R^9$ is the costate or the Lagrange multiplier. Substituting the control law equation (37) into Eq. (31) gives the closed-loop system

$$\dot{x_a} = \left[A_a(\boldsymbol{x}_a) - B_a\epsilon^{-1}B_a^T P(\boldsymbol{x}_a)\right]\boldsymbol{x}_a \doteq A_c(\boldsymbol{x}_a)\boldsymbol{x}_a \tag{40}$$

The closed-loop matrix $A_c(x_a)$ is guaranteed to be Hurwitz at every $\boldsymbol{x}_a \in \Omega$ from the Riccati equation theory.[34] Because the elements of $A_a(\boldsymbol{x}_a)$ are smooth functions, by expanding $A_c(\boldsymbol{x}_a)$ about $\boldsymbol{x}_a = 0$ and using the mean value theorem, one can show that the equilibrium point $\boldsymbol{x}_a = 0$ of Eq. (40) is asymptotically stable. The performance of the closed-loop system depends on the matrix and the weighting matrices $Q_a(\boldsymbol{x}_a)$ and ϵ. In synthesizing the control law equation (37), the estimated state $\hat{\boldsymbol{x}}_a$ instead of $\boldsymbol{x}_a$ is used for feedback.

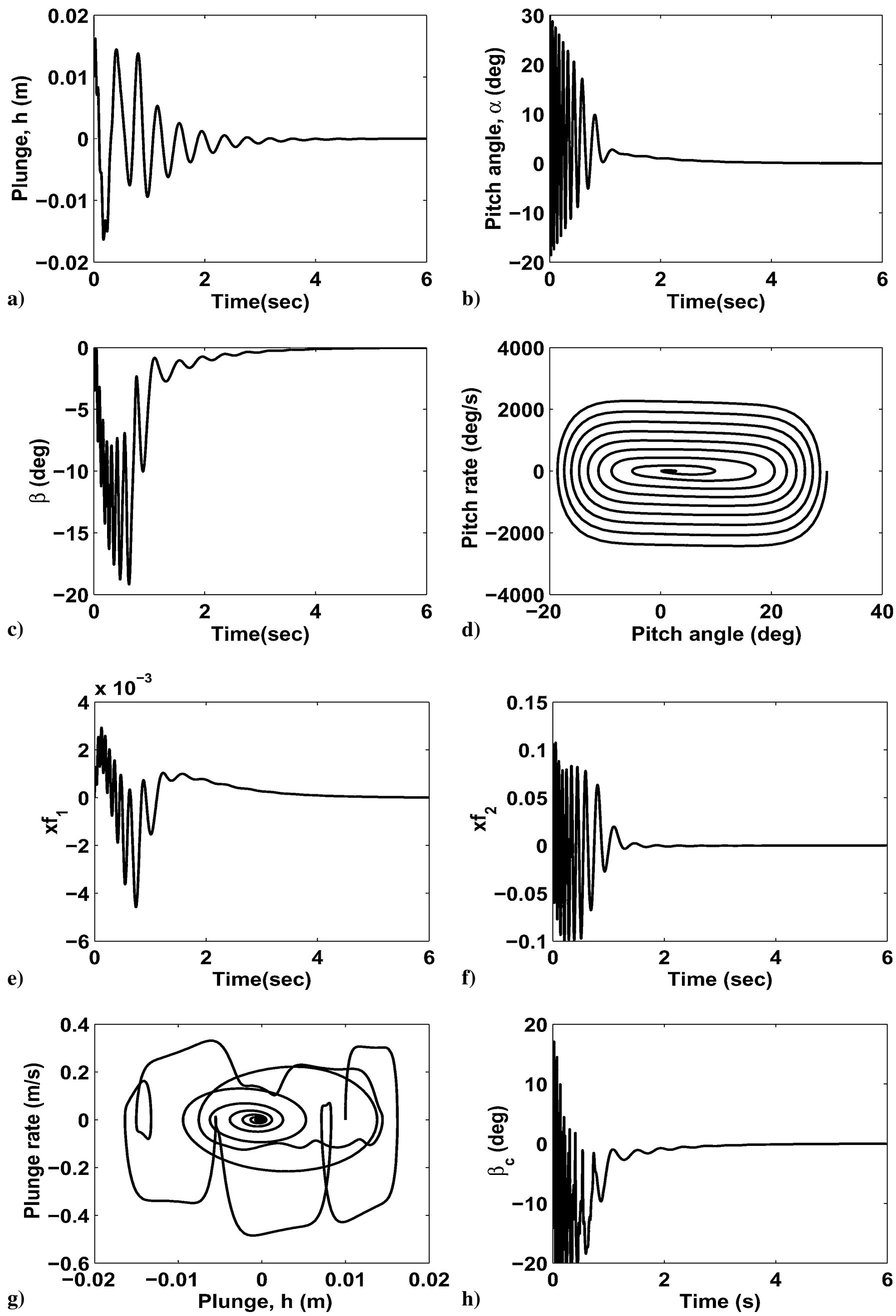

Fig. 3 Stabilization of the system, $a = -0.7$, $u = 20$ (m/s): a) plunge displacement (m); b) pitch angle (deg); c) surface deflection β (deg); d) phase plane plot α (deg)–$\dot{\alpha}$ (deg/s); e) filter state x_{f1}; f) filter state x_{f2}; g) phase plane plot $h(m)$–$\dot{h}$ (m/s); and h) control input β_c (deg).

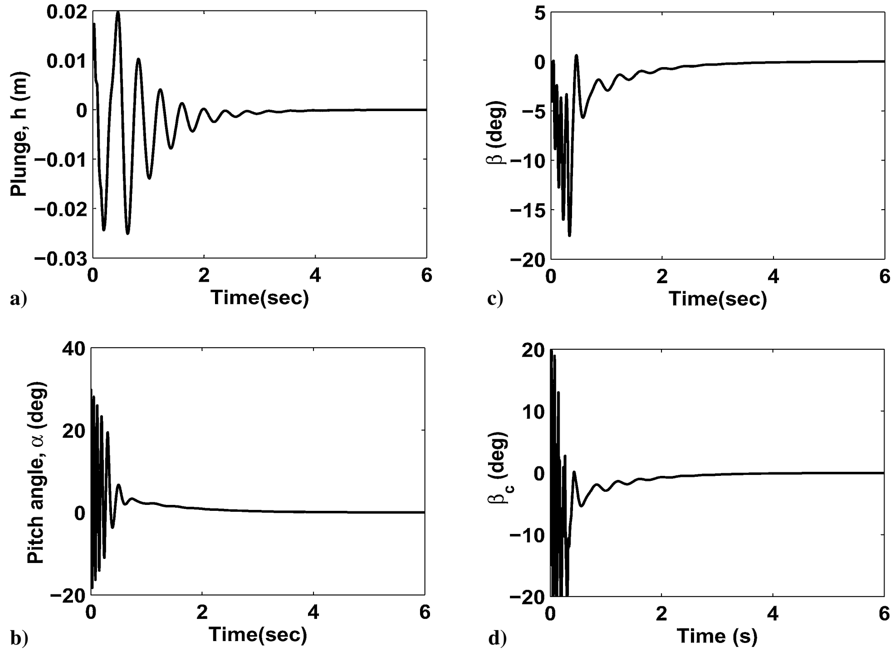

Fig. 4 Stabilization of the system, $a = -0.8$, $u = 30$ (m/s): a) plunge displacement (m); b) pitch angle (deg); c) surface deflection β (deg); and d) control input β_c (deg).

IV. Simulation Results

In this section, the simulation results are presented. The model parameters are taken from Refs. 16–18 and are collected in the Appendix. Results are presented for two sets, (S_1) ($u = 20$ (m/s) $a = -0.7$) and (S_2) ($u = 30$ (m/s), $a = -0.8$), of the flow velocity and parameter a. For simulation, the control input β_c has been limited to $\beta_{\mathrm{cm}} = 20$ (deg).

The initial condition of the model equation (1) is $\boldsymbol{x}(0) = [0.01\text{ (m)}, 30\text{ deg}, 0, 0, 1\text{ (deg/s)}, 0, 0, 0.1]^T$ and the estimator's initial state $\hat{\boldsymbol{x}}(0)$ is $[0.01\text{ (m)}, 30\text{ deg}, 0, 0, 0, 0, 0, 0]^T$. To obtain good responses in the closed-loop system, proper choice of the weighting matrices for the observer and controller is essential. Although there does not exist any systematic method for their choice, in general, a larger penalty on the state vector in the performance index causes faster convergence of the state vector but requires a larger control input.[34] But a choice of a large weighting parameter for the control input yields slow responses and requires a small control magnitude. Here these weighting matrices have been selected after several trials and by observing the simulated responses. For the observer design, the weighing matrices chosen are $Q_0 = 100 I_{8\times 8}$ and $R_0 = 5 I_{3\times 3}$. The weighting matrices for the controller design are $Q = 20 I_{8\times 8}$, $R = 8$, and $\epsilon = 0.01$. The open-loop system has two unstable poles at $1.1917 \pm j14.0002$ for (S_1) and at $1.8862 \pm j17.2562$ for (S_2) and the remaining poles are stable. The open-loop response for each case shows limit cycle oscillations. The plots for case (S_1) are shown in Fig. 2, which show that after an initial transient the pitch angle and the plunge displacement trajectories converge to limit cycles.

A. Case A: Feedback Control for S_1

The complete closed-loop system including the model (1), the observer equation (23), and the suboptimal controller equation (37) for case S_1 is simulated. The responses are shown in Fig. 3. It is observed that the state vector converges to the origin. The response time is on the order of 3–4 s. Figure 3 shows that the filter states x_{f1} and x_{f2} also converge to zero. In the transient period, β_c saturates. It is pointed out that constraining the input β_c provides flexibility in limiting the magnitude of the control-surface deflection as well. Here β remains within 20 deg. It is noted that unlike the feedback linearizing control technique, the SDRE method permits the designer to shape the plunge and pitch responses simultaneously by the choice of the weighting matrices in the performance index.

B. Case B: Feedback Control for S_2

Simulation is performed for the condition S_2 ($u = 30$ (m/s), $a = -0.8$). The initial conditions and controller parameters of case A are retained for simulation. Selected responses are shown in Fig. 4. In the transient period, plunge and pitch responses are oscillatory. It is observed that the plunge displacement, the pitch angle, and the filter states converge to zero. The maximum control-surface deflection β is less than 18 deg and the control input β_c saturates during a segment of the transient period.

Extensive simulations have been performed for other values of the flow velocities and elastic axis locations, and it has been observed that the controller accomplishes flutter control in each case. To this end, a comparison of the SDRE method with other nonlinear design techniques is appropriate. It is found that unlike the feedback linearization control and adaptive feedback linearization approaches of Refs. 17–20 and 23–25 and adaptive variable structure control,[22] the SDRE method is applicable for all values of u and a even if the zero dynamics are unstable. Furthermore, in contrast to these published works, the flexibility in the choice of the weighting matrices in the performance index can be used to shape both the plunge and pitch response characteristics. The controllers designed using the feedback linearization technique give poor responses when the zero dynamics are weakly stable and fail completely if the zero dynamics are unstable. Of course, aeroelastic models have unstable zero dynamics for ceration values of u and a. When the zeros of the linearized model in the two cases (S_1) and (S_2) are computed, it is found that the transfer function has two unstable zeros if the plunge displacement is the output variable. Therefore, it is not possible to design a feedback linearizing flutter-control system based on the plunge displacement as an output variable because the residual pitch-angle response will diverge in the closed-loop system. Yet another advantage of the SDRE method over the methods of these published works is that hard constraints on the control input are included in the design process. However, unlike the adaptive controllers of Refs. 20 and 22–25, the SDRE method requires knowledge of system parameters. Furthermore, one must solve the Riccati equation pointwise along the trajectory of the system, and this requires relatively large computation compared to the feedback linearization technique.

V. Conclusions

In this paper, control of a prototypical aeroelastic wing section with structural pitch and plunge nonlinearities using a single control surface was considered. The model includes unsteady aerodynamics. For the purpose of design, a hard constraint on the control input was introduced. For the controller synthesis, only the plunge displacement, pitch angle, and control-surface deflection were measured. A suboptimal nonlinear control law based on the state-dependent Riccati equation method was derived. An observer was designed to obtain estimates of unavailable state variables for feedback. In the closed-loop system including the observer, asymptotic regulation of the state vector to zero was accomplished. Simulation results were presented that showed that flutter suppression can be achieved for different flow velocities and elastic axis locations even when hard constraint is imposed on the control input.

Appendix: System Parameters

The system parameters for simulation have been taken from Refs. 16 and 17: $b = 0.135$ m, $m_w = 1.662$ kg, $c_h = 27.43$ Ns/m, $c_\alpha = 0.036$ Ns, $\rho = 1.225$ kg/m^3, $m_t = 12.387$ kg, $I_\alpha = 0.04325 + m_w x_\alpha^2 b^2$ kg $\cdot$ m^2, $x_\alpha = [0.0873 - (b + ab)]/b$, $T_1 = -0.0630$, $T_4 = -0.4104$, $T_7 = 0.0128$, $T_8 = 0.0964$, $T_{10} = 1.6798$, $T_{11} = 0.8551$, $k_\alpha = 2.82(1 - 22.1\alpha + 1315.5\alpha^2 + 8580\alpha^3 - 17{,}289.7\alpha^4)$ N$\cdot$m/rad, and $k_h = 2844.4 + 255.99h^2$ N/m.

Acknowledgment

The authors thank T. W. Strganac for making the model parameters available for this research.

References

[1] Fung, Y. C., *An Introduction to the Theory of Aeroelasticity*, Wiley, New York, 1955, pp. 207–215.

[2] Dowell, E. H. (ed.), *A Modern Course in Aeroelasticity*, Kluwer Academic, Norwell, MA, 1995, Chap. 1.

[3] Mukhopadhyay, V.,"Historical Perspective on Analysis and Control of Aeroelastic Responses," *Journal of Guidance, Control, and Dynamics*, Vol. 26, No. 5, 2003, pp. 673–684.

[4] Lind, R., and Brenner, M., *Robust Aeroservoelastic Stability Analysis*, Springer-Verlag, New York, 1999, Chap. 9.

[5] Friedmann, P. P., Guillot, D., and Presente, E., "Adaptive Control of Aeroelastic Instabilities in Transonic Flow and Its Scaling," *Journal of Guidance, Control, and Dynamics*, Vol. 20, No. 6, 1997, pp. 1190–1199.

[6] Waszak, M. R., "Robust Multivariable Flutter Suppression for the Benchmark Active Control Technology (BACT) Wind-Tunnel Model," *Journal of Guidance, Control, and Dynamics*, Vol. 24, No. 1, 2001, pp. 147–153.

[7] Scott, R. C., Hoadley, S. T., Wieseman, C. D., and Durham, M. H., "Benchmark Active Controls Technology Model Aerodynamic Data," *Journal of Guidance, Control, and Dynamics*, Vol. 23, No. 5, 2001, pp. 914–921.

[8] Bennett, R. M., Scott, R. C., and Wieseman , C. D., "Computational Test Cases for the Benchmark Active Controls Model," *Journal of Guidance, Control, and Dynamics*, Vol. 23, No. 5, 2000, pp. 922–929.

[9] Mukhopadhyay, V., "Transonic Flutter Suppression Control Law Design and Wind-Tunnel Test Results," *Journal of Guidance, Control, and Dynamics*, Vol. 23, No. 5, 2000, pp. 930–937.

[10] Kelkar, A. G., and Joshi, S. M., "Passivity-Based Robust Control with Application to Benchmark Controls Technology Wing," *Journal of Guidance, Control, and Dynamics*, Vol. 23, No. 5, 2000, pp. 938–947.

[11] Barker, J. M., and Balas, G. J., "Comparing Linear Parameter-Varying Gain-Scheduled Control Techniques for Active Flutter Suppression," *Journal of Guidance, Control, and Dynamics*, Vol. 23, No. 5, 2000, pp. 948–955.

[12] Scott, R. C., and Pado, L. E., "Active Control of Wind-Tunnel Model Aeroelastic Response Using Neural Networks," *Journal of Guidance, Control, and Dynamics*, Vol. 23, No. 6, 2000, pp. 1100–1108.

[13] Guillot, D. M., and Friedmann, P. P., "Fundamental Aeroservoelastic Study Combining Unsteady Computational Fluid Mechanics with Adaptive Control," *Journal of Guidance, Control, and Dynamics*, Vol. 23, No. 6, 2000, pp. 1117–1126.

[14] Prasanth, R. K., and Mehra, R. K., "Control of a Nonlinear Aeroelastic System Using Euler–Lagrange Theory," *Journal of Guidance, Control, and Dynamics*, Vol. 23, No. 6, 2000, pp. 1134–1139.

[15] Ko, J., and Strganac, T. W.,"Nonlinear Adaptive Control of an Aeroelastic System via Geometric Method," AIAA Paper 98-1795, April 1998.

[16] Block, J., and Strganac, T. M., "Applied Active Control for a Nonlinear Aeroelastic Structure," *Journal of Guidance, Control, and Dynamics*, Vol. 21, No. 6, 1998, pp. 838–845.

[17] Strganac, T. W., Ko, J., and Thompson, D. E., "Identification and Control of Limit Cycle Oscillations in Aeroelastic Systems," *Journal of Guidance, Control, and Dynamics*, Vol. 23, No. 6, 2000, pp. 1127–1133.

[18] Ko, J., Kurdila, A. J., and Strganac, T. W., "Nonlinear Control of a Prototypical Wing Section with Torsional Nonlinearity," *Journal of Guidance, Control, and Dynamics*, Vol. 20, No. 6, 1997, pp. 1181–1189.

[19] Ko, J., and Strganac, T. W., "Stability and Control of a Structurally Nonlinear Aeroelastic System," *Journal of Guidance, Control, and Dynamics*, Vol. 21, No. 5, 1998, pp. 718–725.

[20] Ko., J., Strganac, T. W., and Kurdila, A. J., "Adaptive Feedback Linearization for the Control of a Typical Wing Section with Structural Nonlinearity," *Nonlinear Dynamics*, Vol. 18, No. 2, 1999, pp. 289–301.

[21] Sheta, E., Harrand, V. J., Thompson, D. E., and Strganac, T. W., "Computational and Experimental Investigation of Limit Cycle Oscillations of Nonlinear Aeroelastic Systems," *Journal of Aircraft*, Vol. 39, No. 1, 2002, pp. 133–141.

[22] Zeng Y., and Singh, S. N., "Output Feedback Variable Structure Adaptive Control of an Aeroelastic System," *Journal of Guidance, Control, and Dynamics*, Vol. 21, No. 6, 1998, pp. 830–837.

[23] Xing, W., and Singh, S. N.,"Adaptive Output Feedback Control of a Nonlinear Aeroelastic Structure," *Journal of Guidance, Control, and Dynamics*, Vol. 23, No. 6, 2000, pp. 1109–1116.

[24] Singh, S. N., and Wang, L., "Output Feedback Form and Adaptive Stabilization of a Nonlinear Aeroelastic System," *Journal of Guidance, Control, and Dynamics*, Vol. 25, No. 4, 2002, pp. 725–732.

[25] Singh, S. N., and Brenner, M.,"Modular Adaptive Control of a Nonlinear Aeroelastic System," *Journal of Guidance, Control, and Dynamics*, Vol. 26, No. 3, 2003, pp. 443–451.

[26] Bhoir, N. G., and Singh, S. N., "Stabilization of an Aeroelastic System: A Backstepping Design," AIAA Paper 2003-5502, Aug. 2003.

[27] Mracek, C. P., and Cloutier, J. R., "Full Envelope Missile Longitudinal Autopilot Design Using the State-Dependent Riccati Equation Method," AIAA Paper 97-3767, Aug. 1997.

[28] Mracek, C. P., and Cloutier, J. R., "Control Designs for the Nonlinear Bench-Mark Problem via the State-Dependent Riccati Equation Method," *International Journal of Robust Nonlinear Control*, Vol. 8, April 1998, pp. 401–433.

[29] Cloutier, J. R., Mracek, C. P., Ridgely, D. B., and Hammett, K. D., "State Dependent Riccati Equation Techniques: Theory and Applications," Notes from the SDRE Workshop Conducted at the American Control Conf., Philadelphia, June 1998.

[30] Cloutier, J. R., and Stansbery, D. T., "Nonlinear Hybrid Bank-to-Turn/Skid-to-Turn Autopilot Design," AIAA Paper 2001-5929, Aug. 2001.

[31] Singh, S. N., and Yim, W.,"State Feedback Control of an Aeroelastic System with Structural Nonlinearity," *Aerospace Science and Technology*, Vol. 7, No. 1, 2003, pp. 23–31.

[32] Tadi, M., "State-Dependent Riccati Equation for Control of Aeroelastic Flutter," *Journal of Guidance, Control, and Dynamics*, Vol. 26, No. 6, 2003, pp. 914–917.

[33] Theodorsen, T., "General Theory of Aerodynamic Instability and Mechanism of Flutter," NACA Rept. 496, 1935.

[34] Sivan, R., *Linear Optimal Control Systems*, Wiley, New York, 1972, Chap. 3.